MADRID
inter.noise 2019
June 16 - 19
NOISE CONTROL FOR A BETTER ENVIRONMENT

Propeller/rotor sound scattered by great extension surfaces

Poggi, Caterina[1]
Roma Tre University, Department of Engineering
Via della Vasca Navale 79, 00146 Rome (Italy)

Testa, Claudio[2]
CNR-INM, Institute of Marine Engineering
Via di Vallerano 139, 00128 Rome (Italy)

Bernardini, Giovanni[3]
Roma Tre University, Department of Engineering
Via della Vasca Navale 79, 00146 Rome (Italy)

Pasquali, Claudio[4]
Roma Tre University, Department of Engineering
Via della Vasca Navale 79, 00146 Rome (Italy)

Gennaretti, Massimo[5]
Roma Tre University, Department of Engineering
Via della Vasca Navale 79, 00146 Rome (Italy)

ABSTRACT

This paper deals with propeller/rotor operating in proximity of a great extension surface, with the aim of analyzing its effects on the emitted acoustic field. Both purely reflecting and purely absorbing surfaces are considered, and the most suitable way to model their presence is examined. To this purpose, first the effect of the surface on the aero/hydrodynamic sources distributed over propeller and rotor blades is investigated by including it, through the mirror image method, in the aero-hydrodynamic simulation. Then, the influence of the surface on the total acoustic field is examined by assuming it as a scattering surface impinged by the pressure field radiated by the propeller/rotor. Potentialities and drawbacks of the different modeling approaches considered are theoretically and numerically investigated.

---

[1]caterina.poggi@uniroma3.it
[2]claudio.testa@cnr.it
[3]g.bernardini@uniroma3.it
[4]claudio.pasquali@uniroma3.it
[5]m.gennaretti@uniroma3.it

Keywords: Aeroacoustic, hydroacoustic, acoustic scattering
I-INCE Classification of Subject Number: 23

1. INTRODUCTION

In the last decades, the radiated noise prediction has become a crucial issue both in helicopter and marine vehicle design and operational guidelines. Indeed, the increasingly demanding constraints in terms of environmental impact, certification rules, civil and military requirements, on-board comfort, make the propeller/rotor noise generation and propagation one of the most important tasks for helicopter and shipbuilding industries.

This growing interest is proven by the great amount of works concerning aeroacoustic and hydroacoustic analysis of rotor/propeller currently available in the literature (see for instance Refs. [1-8]). However, there is a lack of investigations about the acoustic effect of solid ground or sea surface when their presence might significantly alter the radiated noise field. This may occur in a wide range of engineering applications. For instance, several helicopter missions (like SAR operations) may require low-altitude flight and hovering greatly acoustically affecting neighboring areas. In this case, a significant role in the noise pattern produced by the rotorcraft is played by the aerodynamic/aeroacoustic interaction with nearby obstacles like ground surface and buildings. Similarly, the noise field generated by ship propellers may be strongly affected by the presence of ship hull and sea surface.

In such operating conditions the effect field might be taken into account. Several approaches with different level of accuracy have been proposed to capture the effect of close surfaces on the aero/hydroacoustic of rotors. A ray tracing approach for the evaluation of helicopter noise propagation can be applied when the distance rotorcraft-obstacle is big enough (see, for instance, Refs. [9-10]). Methodologies based on the solution of the wave equation with boundaries taking into account presence and actual shape of obstacles have been also presented and applied [11]. In addition, it is possible to estimate the surface noise effect through a ratio coefficient defined as the ratio between scattered and incident wave amplitudes (see Ref. [12]). Finally, a further approach would consist of applying the image method [13–15] that provides a more accurate simulation of the surface effects, although requiring the inclusion of a specular source of sound (propeller/rotor), and hence additional computational costs.

This paper is focused on the assessment of methodologies for the prediction of noise generated by helicopter rotors and marine vehicle propellers operating nearby great extension surfaces (ground or sea surfaces). These are treated as purely reflective or absorbing for the acoustic signal. Two approaches for the simulation of rotor-ground and propeller-sea surface aero-hydrodynamic and aero-hydroacoustic interactional effects are presented and discussed. The simplest one (referred to as non-interactional method) the rotor/propeller is assumed as a fluid-dynamically isolated body that generates an incident noise field scattered by the surface [16–18]. Thus, in this case, the surface is considered only in the acoustic analysis and the scattered contribution is evaluated through a scattering model or by the mirror image method [19, 20]. In the second approach (interactional method), more accurate but also more computational costly, the surface is included both in aero-hydrodynamic and acoustic analyses. The fluid dynamic simulation that takes into account the surface presence by the mirror image method. The acoustic analysis is performed by radiating the noise sources by both rotor and its specular image.

The paper is structured as follows: first, Section 2, the theoretical/numerical models used for the aero/hydrodynamic and acoustic analysis will be briefly described; then, Section 3, the results of the numerical investigations concerning the rotor-ground and propeller-sea surface configurations are presented, with the aim of highlighting the influence of the close surface on noise patterns (if any), as well as to identify the most suited way of modeling its presence for aero-hydroacoustic applications.

2. THEORETICAL MODELS

In this section aero/hydrodynamic, acoustic and scattering models are briefly described. The aero-hydrodynamic formulation for inviscid flows around lifting/thrusting bodies is numerically implemented by a Boundary Element Method, and provides the input data for the acoustic scattering/radiation solvers considered in the paper.

2.1. Aero-hydrodynamic solver

For a lifting/thrusting body in arbitrary motion with respect to the undisturbed medium, let us consider the unsteady, incompressible flow around it assumed to be quasi-potential (namely, potential everywhere except on the wake surface defined as the locus of the material points that have come in contact with the body). The velocity potential field, φ, such that $\boldsymbol{v} = \nabla\varphi$, may be represented by the following boundary integral equation [21]:

$$E(\boldsymbol{x})\,\varphi(\boldsymbol{x},t) = \int_{S_B}\left[G\frac{\partial\varphi}{\partial n} - \varphi\frac{\partial G}{\partial n}\right]dS(\boldsymbol{y}) - \int_{S_W}\Delta\varphi\,\frac{\partial G}{\partial n}\,dS(\boldsymbol{y}) \tag{1}$$

where S_B and S_W are body and wake surfaces, respectively, whereas the field function, $E(\boldsymbol{x})$, is equal to 0, 1/2, 1, if $\boldsymbol{x}$ is inside, on, or outside S_B, respectively.

Thus, the velocity potential is described as the combined effect of distributions of sources and doublets over the body surface and of doublets over the wake surface. In Equation (1), $G = -1/4\pi\, r$ is the free-space, unit-source solution of the three-dimensional Laplace equation, with $r = \|\boldsymbol{r}\| = \|\boldsymbol{x} - \boldsymbol{y}\|$, while $\Delta\varphi$ denotes the potential jump across the wake surface, known from past history of potential discontinuity at the blade trailing edge through the Kutta-Joukowski condition [22,23]. In addition, the impermeability boundary condition yields $\partial\varphi/\partial n = \boldsymbol{v}_B \cdot \boldsymbol{n}$, with $\boldsymbol{v}_B$ representing the body velocity and $\boldsymbol{n}$ its outward unit normal.

Equation (1) is solved numerically by boundary elements, *i.e.* by discretizing S_B and S_W into quadrilateral panels, assuming φ, $\partial\varphi/\partial n$ and $\Delta\varphi$ to be piecewise constant and imposing that the equation be satisfied at the center of each body element (collocation method).

Note that, Eq. (1) is strictly applied for the hydrodynamic analysis of propellers, whereas the aerodynamic analysis of helicopter rotors, if subject to strong wake-body interaction effects, is performed through a suited free-wake solver based on an integral formulation derived as an extension of that in Eq. (1) [24,25]. Specifically, the latter is inspired by the observation that the instabilities arising in the numerical formulation derived from Eq. (1) when wake panels are too close to or impinge the body, would be eliminated by replacing the doublet distributions with equivalent ring thick vortices (namely, Rankine vortices) [24,25].

Once the velocity potential $\varphi(\boldsymbol{x},t)$ is known through the aero/hydrodinamic solver, the pressure can be evaluated everywhere through the Bernoulli theorem. Specifically, the perturbation, p', induced at an arbitrary location $\boldsymbol{x}$ in the fluid domain is given by

$$p'(\boldsymbol{x},t) = -\rho_0\left(\frac{\partial\varphi}{\partial t} - \boldsymbol{v}_B\cdot\nabla\varphi + \frac{1}{2}|\nabla\varphi|^2\right) \tag{2}$$

The presence of a close obstacle proposes a challenging interference aerodynamic problem to deal with. Two approaches could be followed: (*i*) inclusion of the external surface as a boundary of the flowfield, for arbitrarily shaped obstacles (Bounded-Domain Method-BDM); (*ii*) if the obstacle consists of a wide flat surface, inclusion of a twin rotor/propeller in the mathematical model symmetrically placed with respect to the surface, such to produce the same effects that would be generated by the surface (Mirror Image Method-MIM).

Due to the well known numerical complexity in satisfying the impermeability boundary condition when a wake closely interacts with a body [26], and considering that the objective of the paper is the examination of great extension surface noise effects, here the MIM is applied [27]. It is widely used in aeronautics and marine applications, and has been successfully applied by the authors in the recent past against experimental data [20, 28].

2.2. Acoustic solver

The aerocoustic effects of a close, flat, great-extension boundary surface, S_S, may be taken into account either applying the MIM or considering it as a scattering surface. For an arbitrarily shaped surface, only the second approach is efficiently applicable.

In the first case, the radiated noise is evaluated through the Farassat 1A boundary integral formulation [29] for the solution of the Ffowcs Williams and Hawkings equation applied to the rotor blades and their twins that are specular with respect to the boundary surface. Specifically, the acoustic pressure field is given as the superposition of the thickness noise, p'_T, depending on body geometry and kinematics,

$$4\pi p'_T(\boldsymbol{x},t) = \int_{S_{BM}}\left[\frac{\rho_0\dot{v}_n}{r|1-M_r|^2}\right]_\tau dS(\boldsymbol{y}) + \int_{S_{BM}}\left[\frac{\rho_0 v_n(r\dot{\boldsymbol{M}}\cdot\hat{\boldsymbol{r}} + c_0M_r - c_0M^2)}{r^2|1-M_r|^3}\right]_\tau dS(\boldsymbol{y}) \tag{3}$$

and the loading noise, p'_L, related to the distribution of pressure over body surfaces,

$$\begin{aligned}4\pi p'_L(\boldsymbol{x},t) = \frac{1}{c_0}\int_{S_{BM}}\left[\frac{\dot{\tilde{p}}\boldsymbol{n}\cdot\hat{\boldsymbol{r}} + \tilde{p}\dot{\boldsymbol{n}}\cdot\hat{\boldsymbol{r}}}{r|1-M_r|^2}\right]_\tau dS(\boldsymbol{y}) + \int_{S_{BM}}\left[\frac{\tilde{p}\boldsymbol{n}\cdot\hat{\boldsymbol{r}} - \tilde{p}\boldsymbol{M}\cdot\boldsymbol{n}}{r^2|1-M_r|^2}\right]_\tau dS(\boldsymbol{y})\\ + \frac{1}{c_0}\int_{S_{BM}}\left[\frac{\tilde{p}\boldsymbol{n}\cdot\hat{\boldsymbol{r}}}{r^2|1-M_r|^3}r\dot{\boldsymbol{M}}\cdot\hat{\boldsymbol{r}}\right]_\tau dS(\boldsymbol{y}) + \int_{S_{BM}}\left[\frac{\tilde{p}\boldsymbol{n}\cdot\hat{\boldsymbol{r}}}{r^2|1-M_r|^3}(M_r - M^2)\right]_\tau dS(\boldsymbol{y})\end{aligned} \tag{4}$$

where $S_{BM} = S_B \cup S_M$, with S_M denoting the surface of the specular rotor blades. In Eqs. (3) and (4), $\hat{\boldsymbol{r}} = \boldsymbol{r}/r$ is the unit vector along the source-observer direction, c_0 and ρ_0 are, respectively, speed of sound and density in the undisturbed medium, $\tilde{p} = (p - p_0)$ with p_0 representing the undisturbed medium pressure, $\boldsymbol{M} = \boldsymbol{v}_B/c_0$, $M = \|\boldsymbol{M}\|$, $M_r = \boldsymbol{M}\cdot\hat{\boldsymbol{r}}$, and $v_n = \boldsymbol{v}_B\cdot\boldsymbol{n}$. Further, $\dot{v}_n$, $\dot{\boldsymbol{n}}$ and $\dot{\boldsymbol{M}}$ denote time derivatives of v_n, $\boldsymbol{n}$ and $\boldsymbol{M}$, observed in a frame of reference fixed with the undisturbed medium. Notation $[...]_\tau$ indicates that these quantities are evaluated at the delayed source time, $\tau = t - \theta$, where θ is the time taken by the signal started from $\boldsymbol{y} \in S_B$ to arrive at $\boldsymbol{x}$ at time t.

When the surface is considered as a noise scatterer, the total noise field, p'_{tot}, is divided into incident and scattered components. The noise emitted by the rotor/propeller is considered as an impinging pressure field which is then scattered by the ground or by the sea surface. The scattering problem is solved through the following boundary integral formulation for the solution, in the frequency domain, of the linear Ffwocs Williams and Hawkings equation for the scattered pressure field [16]

$$\tilde{p}'_s(\boldsymbol{x}, k) = -\int_{S_S} \left[\frac{\partial G}{\partial n} - jk\, G\, \frac{\partial r}{\partial n} \right] (\tilde{p}'_i + \tilde{p}'_s)\; e^{-jkr}\, \mathrm{d}S(\boldsymbol{y}) \tag{5}$$

where $\tilde{p}'_s$ and $\tilde{p}'_i$ denote the scattering pressure and the incident pressure respectively, and $k = \omega/c_0$ the wave number of the impinging field. If the scattering surface is fixed with the undisturbed medium, $G = -1/4\pi r$. For the solution of Eq. (5), the boundary conditions to be applied consist of the incident pressure distribution over S_S.

From considerations inspired by the MIM approach, it can be readily inferred that over purely reflecting infinite surfaces, $\tilde{p}'_s = \tilde{p}'_i$ (namely, $p'_{tot} = 2\, p'_i$), whereas over purely absorbing infinite surfaces, $\tilde{p}'_{tot} = 0$ and hence, $\tilde{p}'_s = -\tilde{p}'_i$ [15].

3. NUMERICAL RESULTS

The theoretical models described above are applied for the aero-hydroacoustic analysis of rotors and propellers operating in proximity of great extension, purely reflective and absorbing, flat surfaces. The following numerical investigations are aimed at assessing the influence of the surface on the noise field focusing, in particular, on (i) a hovering helicopter rotor parallel to the ground, with wake impinging on it, and (ii) a marine propeller moving axially along a rectilinear trajectory parallel to the free sea surface (no wake-surface impact).

Specifically, the investigation concerns the role played by the aero-hydrodynamics interference effects in acoustic predictions. Namely, pressure fields generated by rotor/ground and propeller/sea surface configurations with and without inclusion of the surface presence in the evaluation of the input pressure for the acoustic radiation model are compared. Note that, non-interference aero-hydrodynamics means analysis of isolated rotor/propeller in unbounded space, whereas the MIM approach is used for the inclusion of interference effects.

In addition, the attention is focused on the different acoustic role played by the boundary surface in the near and in the far field (assessment of the different surface acoustic interference effects for different distances of the observer from it).

All of the results are presented in terms of incident, scattered and total pressure fields, as well as shielding factor (defined as the ratio between total and incident pressure).

3.1. Helicopter rotor in-ground-effect aeroacoustics

Let us consider a scaled model helicopter rotor hovering on a flat ground surface parallel to the rotor disk. The rotor characteristics are given in Table 1), the hub is one rotor radius distant from the ground and the observers lie on a hemisphere of radius d centered on the ground, at the point beneath the rotor hub.

radius (R)	0.408 m
chord	0.044 m
angular speed	2100 rpm
number of blades	2

Table 1: helicopter rotor data.

First, Fig. 1 compares, on a hemisphere of radius $d = 5R$, the rotor acoustic disturbances predicted through Eqs. (3) and (4) for $S_{BM} \equiv S_B$ (incident acoustic field), derived from aerodynamic input data determined with and without inclusion of the close surface boundary effects. The frequency component considered is that related to the first blade passage frequency, namely, $k = \omega/c_0 = 1.29$. Note that θ denotes the azimuth angle defining rotations about the rotor axis, whereas ϕ denotes the elevation angle with respect to the ground, with $\phi = \pi/2$ corresponding to the pole of the hemisphere at the intersection with the rotor axis. This picture clearly shows that the effect of the surface is negligible in terms of noise directly emitted by the rotor, and hence the simpler isolated rotor configuration can be conveniently used (at least for the rotor/surface configuration examined here) for the determination of the incident pressure field to be applied in the sound scattering formulation.

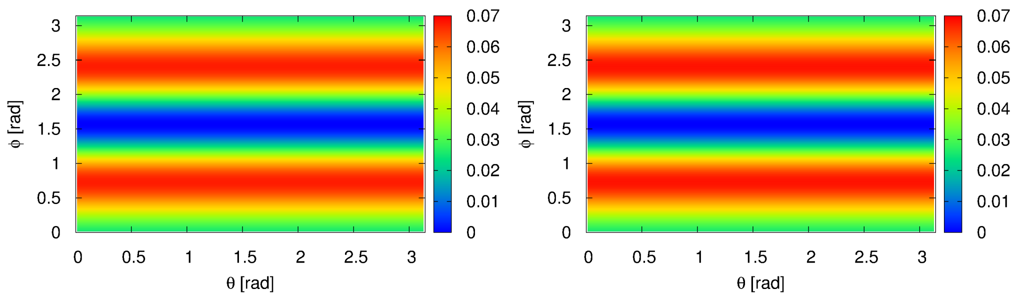

(a) isolated rotor (b) rotor/surface configuration

Figure 1: Incident acoustic disturbance with and without interference aerodynamic effects; $d = 5R$, $k = 1.29$.

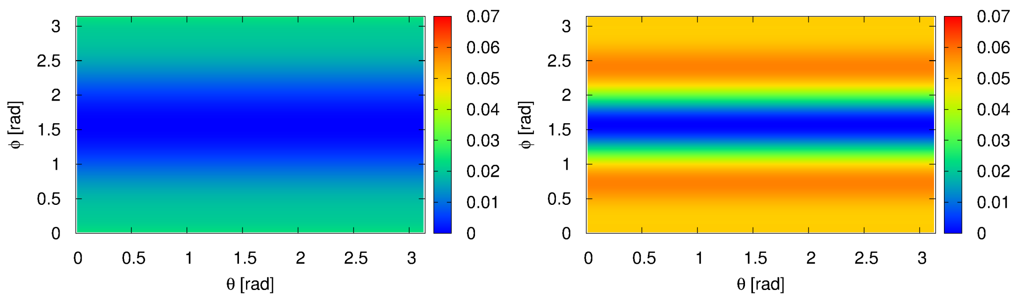

(a) scattered pressure (b) total pressure

Figure 2: Ground acoustic disturbance for purely reflective surface; $d = 5R$, $k = 1.29$.

Next, for $d = 5R$ and $k = 1.29$, Fig. 2 shows the contour plots of the scattered and total pressure fields for a purely reflective ground, corresponding to the incident field illustrated in Fig. 1. It demonstrates that, although the presence of the ground in the aerodynamic analysis produces negligible effects on the evaluation of the noise field directly radiated by the rotor, at least for the rotor-ground distance examined, it significantly affects the total acoustic field (compare Figs. 1 and 2(b)). These considerations remain valid also for different observer positions, as demonstrated by numerical investigations not shown here for the sake of conciseness.

Note that the scattered pressure fields shown in Fig. 2(a) is determined by the MIM approach. However, the same results have been obtained by the formulation in Eq. (5) through application of suitable surface discretization mesh and extension (these results are not shown here for the sake of conciseness).

Next, the acoustic impact of the surface presence is investigated letting the surface-observer distance increase. The results in Fig. 3 show the computed shielding factor for three different surface-observer distances. It demonstrates that the relative acoustic

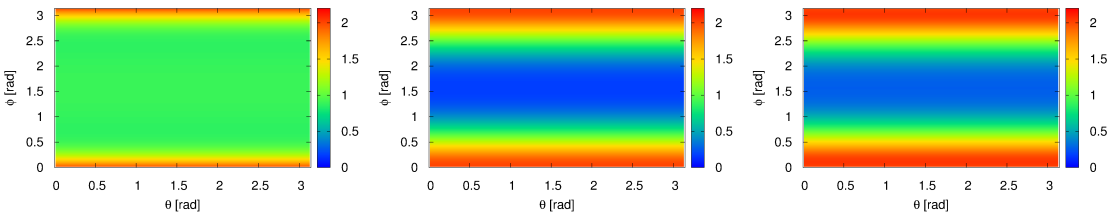

(a) $d = 5R$ (b) $d = 25R$ (c) $d = 125R$

Figure 3: Influence of observer-surface distance on shielding factor. Purely reflective surface, $k = 1.29$.

impact of ground increases with the distance. Indeed, for the minor distance considered, not negligible acoustic effects of the surface are confined in a very small region bordering the ground, outside of which the shielding factor is almost everywhere equal to one. Instead, as the distance increases, the scattered contribution is significant for almost all the observers, making the total pressure field considerably different from that radiated by the rotor in the unbounded space. Specifically, in the far field scattered and incident components are combined in such a way that, near the ground, the total pressure is twice greater than that radiated by the isolated rotor (these observers receive identical signals from the rotor and its specular twin), whereas it tends to be negligible above the rotor disk (indeed, as the distance of observers in the neighborhood of rotor axis increases, rotor and specular twin tend to be perceived as overlapping, with their dominant noise contribution -related to doublet distributions- of opposite sign).

3.2. Propeller hydroacoustic analysis

Here, the hydroacoustic effects of the sea surface (assumed both as purely reflective and purely absorbing) are examined.

First of all, as in the previous section, the first analysis concerns the impact of hydrodynamic propeller/surface interference effects on the radiated noise. For this investigation the case-study propeller described in Table 2 is considered in uniform axial motion, parallel to the sea surface. The distance between its hub and the surface is equal to $3R$.

radius (R)	0.746 m
chord	0.297 m
angular speed	2500 rpm
number of blades	3
advance ratio	2.7

Table 2: Three-bladed propeller data.

For two blade sections located at $r/R = 0.35$ and $r/R = 0.8$, Fig. 4 presents the comparisons of the pressure perturbations determined by hydrodynamic predictions including and not including surface interference effects. These figures prove that, akin to

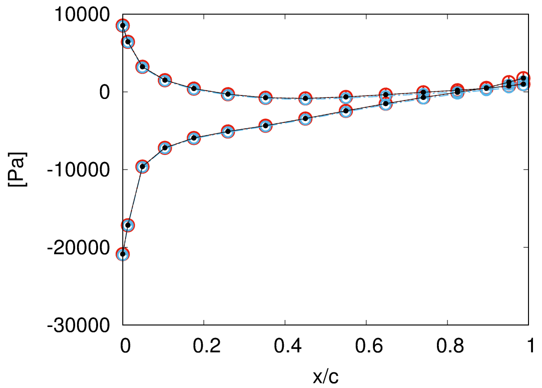

(a) $r/R = 0.35$

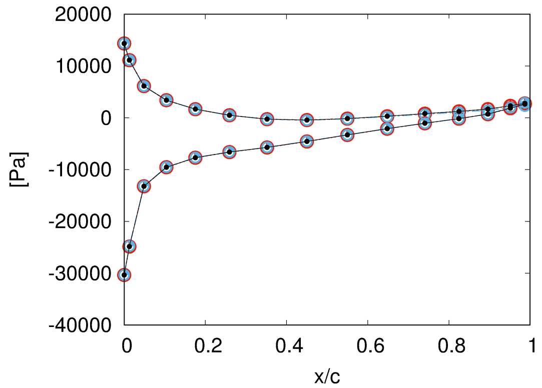

(b) $r/R = 0.8$

Figure 4: Chordwise pressure distribution: no hydrodynamic interference (black circles), hydrodynamic interference from reflective surface (red circles), hydrodynamic interference from absorbing surface (blue circles).

the rotor case, both for purely reflecting and absorbing surfaces the pressure field over the propeller blades is not appreciably affected by surface interference effects.

In the following, for the sake of simplicity, hydrodynamic predictions are performed without inclusion of surface interference effects.

Next, the 4-bladed marine propeller INSEAN-E1637 [30] in uniform axial motion parallel to the sea surface is considered (see Table 3). Its distance to the surface is equal to $2R$, with the observers lying on a rectangular plane area parallel to the sea surface, distant b from it, with size of sides equal to $70R$ (along the propeller axis) and $28R$.

radius (R)	0.1165 m
angular speed	480 rpm
number of blades	4
advance ratio	0.9

Table 3: Four-bladed marine propeller data.

Figures 5 and 6 present the shielding factor predicted on the observer plane placed at three different distances from the surface, for $k = 0.134$ (first blade passage frequency), for purely reflective and absorbing sea surfaces, respectively (note that, in this case, the acoustic fields are evaluated directly from the potential field solution by the application of the Bernoulli theorem). For both types of sea surfaces examined, the greater the

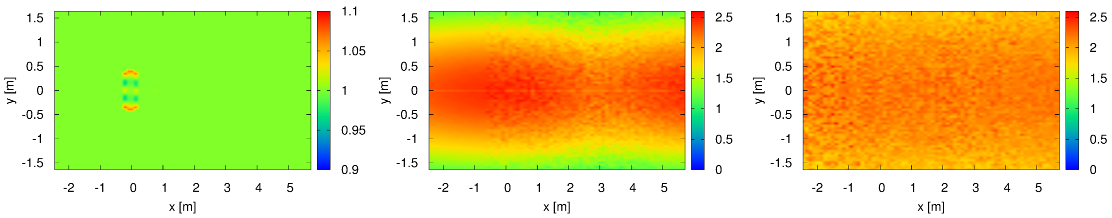

(a) $b = 4R$ (b) $b = 50R$ (c) $b = 100R$

Figure 5: Shielding factor for a purely reflective surface. $k = 0.134$.

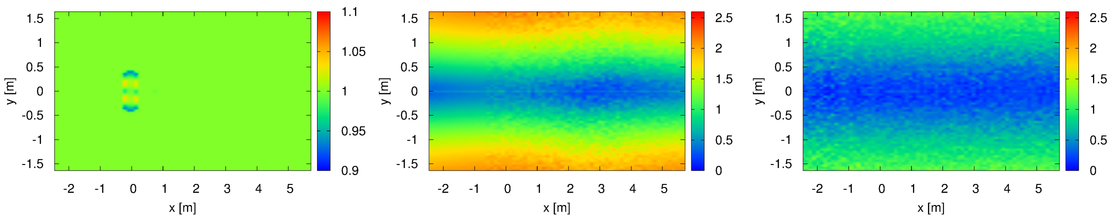

(a) $b = 4R$ (b) $b = 50R$ (c) $b = 100R$

Figure 6: Shielding factor for a purely absorbing surface. $k = 0.134$.

observers-propeller distance, the greater the surface acoustic effect. Indeed, when the microphones are very close to the propeller, the only noticeable acoustic effect is that directly radiated by the propeller (namely, the incident pressure), whereas for increasingly distance the scattered contribution increases, becoming significant from a distance of about $50R$ (see Figs. 5(b) and 6(b)). Moreover, the comparison of Figs. 5 and 6 shows that reflecting and absorbing sea surfaces produce quite different acoustic effects. Indeed, for observer placed at distances where the scattered contribution is significant, for purely reflective surface it is observed an evident increase of pressure disturbance in the region below propeller and wake, whereas for the purely absorbing surface, the region below propeller and wake is where scattered and incident acoustic disturbances tend to counterbalance, while they remain of the same order of magnitude for observers further away from the propeller axis.

4. CONCLUSIONS

Aero/hydroacoustics of rotors and propellers operating near great-extension surfaces (ground/sea surface) has been investigated. Purely reflecting and purely absorbing surfaces have been considered. Both the effect of the surface on rotor/propeller aero/hydrodynamics and its influence on the corresponding acoustic near/far field have been examined. For the rotor/propeller-surface configurations considered, the main outcomes of the accomplished numerical investigation are: (i) noise radiated by rotor/propeller is almost unaffected by the presence of the surface, and hence incident acoustic fields may be conveniently determined by isolated rotor/propeller aero/hydrodynamics solvers; (ii) the presence of the surface may significantly affect the acoustic field, both when considered purely reflecting and when assumed as a purely absorbing surface; (iii) the acoustic effects of the surface tend to increase with the distance from the rotor, in that the very near field is dominated by the incident noise directly radiated by the rotor/propeller.

5. REFERENCES

[1] Strawn, R. C., Biswas, R. adn Lyrintzis, A. S. "Helicopter noise predictions using Kirchhoff methods". *Journal of Computational Acoustics*, 4(03), 321-339. 1996

[2] Farassat, F. and Succi, G. P. "The prediction of helicopter rotor discrete frequency noise". In American Helicopter Society, Annual Forum, 38th, Anaheim, CA, May 4-7, 1982, Proceedings.(A82-40505 20-01) Washington, DC, American Helicopter Society, 1982, p. 497-507. (pp. 497-507). 1982.

[3] Gennaretti, M., Bernardini, G., Sander, H., Scandroglio, A., Riviello, L., Paolone, E., 'Experimental/Numerical Acoustic Correlation of Helicopter Unsteady Manoeuvres,' *42nd European Rotorcraft Forum*, Lille, France, September 5–8. 2016.

[4] Wei, Yingsan, et al. "Scattering effect of submarine hull on propeller non-cavitation noise." Journal of Sound and Vibration 370 (2016): 319-335

[5] Testa C, Greco L. (2018). "Prediction of Submarine Scattered Noise by the Acoustic Analogy". Journal of Sound and Vibration, vol. 426, 21 p. 186-218, ISSN: 0022460X, doi: 10.1016/j.jsv.2018.04.011

[6] Ianniello, S., Muscari, R., Di Mascio, A. (2013) "Ship underwater noise through the acoustic analogy Part I: Nonlinear analysis of a marine propeller in a uniform flow." J. Mar. Sci. Tech., 18, pp.547-570.

[7] Testa, C., Porcacchia, F., Greco, L., Muscari, R. (2018) "Effectiveness of Boundary Element Method Hydrodynamic Data for Propeller Hydroacoustic,", 3 rd International Meeting on Propeller Noise and Vibration, AYOCOL 18, Istanbul

[8] Testa C., Greco L., Salvatore F., "Computational Approaches for the Prediction of Hull Pressure Fluctuations" Proceedings of the 11th International Symposium on Practical Design of Ships and Other Floating Structures (PRADS 2010). Rio de Janeiro, Brasile, 19-24 Settembre 2010, vol. 1, ISBN/ISSN: 978-85-285-0140-7.

[9] Vorländer, M., "Simulation of the transient and steady-state sound propagation in rooms using a new combined ray-tracing/image-source algorithm", *The Journal of the Acoustical Society of America*, 86(1), 172-178. 1989

[10] Le Bot, A. and Bocquillet, A. "Comparison of an integral equation on energy and the ray-tracing technique in room acoustics", *The Journal of the Acoustical Society of America*, 108(4), 1732-1740. 2000.

[11] Casalino, Damiano, Mattia Barbarino, and Antonio Visingardi. "Simulation of helicopter community noise in complex urban geometry." AIAA journal 49.8 (2011): 1614-1624.

[12] Brekhovskikh, Leonid Maksimovich, Yu P. Lysanov, and Jurij P. Lysanov. Fundamentals of ocean acoustics. Springer Science & Business Media, 2003.

[13] Seybert, A. F., Soenarko, B., "Radiation and scattering of acoustic waves from bodies of arbitrary shape in a three-dimensional half space", Journal of vibration, acoustics, stress, and reliability in design, 1988, 110.1: 112-117.

[14] Seybert, A. F., Wu, T. W., "Modified Helmholtz integral equation for bodies sitting on an infinite plane", The Journal of the Acoustical Society of America, 1989, 85.1: 19-23.

[15] Y.-Z.Kehr, C.-Y.Hsin, Y.-C.Sun "Calculations of Pressure Fluctuations on the Ship Hull Induced by Intermittently Cavitating Propellers". Twenty-First Symposium on Naval Hydrodynamics (1997)

[16] Gennaretti, M., and Testa, C., "A Boundary Integral Formulation for Sound Scattered by Moving Bodies,“ *Journal of Sound and Vibration*, Vol. 314, (3-5), 2008, pp. 712-737.

[17] Gennaretti, M., Bernardini, G., Poggi, C., and Testa, C. (2018). "Velocity-Potential Boundary-Field Integral Formulation for Sound Scattered by Moving Bodies". AIAA Journal, 1-11.

[18] Bernardini, G. Testa, C. Gennaretti, M., "Tiltrotor cabin noise control through smart actuators," Journal of Vibration and Control, 22 (1) (2014) 3-17 doi:10.1177/1077546314526919.

[19] Gennaretti, M., Pasquali, C., Cardito, F., Serafini, J., Bernardini, G., and Celi, R., "Dynamic wake inflow modeling in ground effect for flight dynamics applications," *73rd AHS Annual Forum and Technology Display*, Fort Worth, Texas, May, 2017.

[20] Pasquali, C., Serafini, J., Bernardini, G., Gennaretti, M., Milluzzo, J., Davids, S., "Numerical-experimental correlation of rotor flowfield in ground effect," *44th European Rotorcraft Forum*, Delft, Netherlands, September 18-20, 2018.

[21] Morino, L. and Gennaretti, M., "Boundary Integral Equation Methods for Aerodynamics," in: S.N. Atluri (Ed.), Computational Nonlinear Mechanics in Aerospace Engineering, *Progress in Astronautics and Aeronautics*, Vol. 146, AIAA, 1992.

[22] Gennaretti, M., Luceri, L. and Morino, L., "A unified boundary integral methodology for aerodynamics and aeroacoustics of rotors" *Journal of Sound and Vibration*, 200(4):467-489, 1997

[23] Morino, L., Bernardini, G., "Singularities in BIEs for the Laplace equation; Joukowski trailing-edge conjecture revisited", *Engineering analysis with boundary elements*, 25(9):805-818,2001

[24] Gennaretti, M. and Bernardini, G., "Novel Boundary integral formulation for blade-vortex interaction aerodynamics of helicopter rotors", *AIAA Journal*, 45(6): 1169-1176, 2007

[25] Bernardini, G., Serafini, J., Molica Colella, M. and Gennaretti, M. "Analysis of a structural-aerodynamic fully-coupled formulation for aeroelastic response of rotorcraft", *Aerospace Science and Technology*, 29(1): 175-184, 2013

[26] Ploumhans, P., and Winckelmans, G. S., "Vortex methods for high-resolution simulations of viscous flow past bluff bodies of general geometry". *Journal of Computational Physics*, 165(2), 354-406. (2000)

[27] Young, Y. L., and Kinnas, S. A., "Analysis of supercavitating and surface-piercing propeller flows via BEM". *Computational Mechanics*, 32(4-6), 269-280. (2003)

[28] Light, J. S. "Tip vortex geometry of a hovering helicopter rotor in ground effect". *Journal of the American helicopter society*, 38(2), 34-42. 1993

[29] Farassat, F, "Derivation of Formulations 1 and 1A of Farassat", Tech. Rep. TM-2007-214853, NASA, 2007

[30] Di Felice F., Salvatore F., Dymarski P., Pereira F.A., Franchi S., Falchi M., "Deliverable D21.1- Results of model tests on reference configurations" STREAMLINE-FP7-233896, 2011